Journal of Motor Behavior, 1993, Vol. 25, No. 3, 140–152

Control of Trajectory Modifications in Target-Directed Reaching

J. Randall Flanagan
David J. Ostry
Department of Psychology
McGill University

Anatol G. Feldman
Institut de génie biomedical
Université de Montréal and
Institut de réadaptation de Montréal

ABSTRACT. Human reaching movements to fixed and displaced visual targets were recorded and compared with simulated movements generated by using a two-joint arm model based on the equilibrium-point (EP) hypothesis (λ model) of motor control (Feldman, 1986). The aim was to investigate the form of central control signals underlying these movements. According to this hypothesis, movements result from changes in control variables that shift the equilibrium position (EP) of the arm. At any time, muscle activations and forces will depend on the difference between the arm's EP and its actual position and on the limb's velocity. In this article, we suggest that the direction of EP shift in reaching is specified at the hand level, whereas the rate of EP shift may be specified at the hand or joint level. A common mechanism underlying reaching to fixed and displaced targets is proposed whereby the EP of the hand shifts in a straight line toward the *present* target. After the target is displaced, the direction of the hand EP shift is modified toward the second target. The results suggest that the rate of shift of the hand EP may be modified for movements in different parts of the work space. The model, with control signals that vary in a simple fashion over time, is able to generate the kinematic patterns observed empirically.

Key words: equilibrium-point hypothesis, human reaching movement, trajectory modifications

This article explores the control of horizontal reaching movements to fixed and displaced visual targets. The goal is to demonstrate that a two-joint version of the equilibrium-point (EP) hypothesis or λ model (Feldman, 1986) of motor control with simple control signals can account for the kinematics of horizontal reaching movements. According to this model, movements arise as a consequence of shifts in the EP of the motor system mediated by central commands. Muscle activations and forces depend in a time-varying fashion on the difference between the EP and the actual position of the limb.

The model assumes that target-directed arm movements are achieved by shifting the EP of the hand in a straight line toward the target. In this article, we suggest that if a target is displaced, the direction of shift changes such that the hand EP moves toward the new target position. Thus, we propose that a movement to a displaced target is produced by two shifts in the EP, which occur one after the other. This model may be contrasted with other models that suggest that movements to successive targets are composed of planned submovements that are superimposed and overlap in time (e.g., Flash & Henis, 1991; Milner, 1992; Munhall & Löfqvist, 1990). These other models are based on the finding that the kinematics of movements to displaced targets can be produced by the summation of the kinematics of submovements between the successive targets. We suggest that the central commands underlying these kinematic patterns may be applied successively and need not be superimposed. Thus, whereas superposition appears to apply at the level of kinematics, it may not apply at the planning level. Note that our model and the superposition schemes may make similar predictions about kinematics. They differ in that our model incorporates the dynamic mechanisms underlying movement generation.

The model was evaluated by comparing simulated trajectories with actual trajectories of movements made in different regions of space and to fixed and displaced targets. We first review the organization and form of central commands in the single-joint λ model and then consider how these commands are organized in the two-joint λ model.

Correspondence address: David J. Ostry, Department of Psychology, McGill University, 1205 Dr. Penfield Avenue, Montreal, Quebec H3A 1B1, Canada. E-mail address: ostry@motion.psych.mcgill.ca. Present address for J. R. Flanagan: M.R.C. Applied Psychology Unit, 15 Chaucer Road, Cambridge, CB2 2EF, U.K.

Single-Joint Control

The λ model proposes that central commands are associated with changes in λ, the muscle's threshold length for motoneuron (MN) recruitment. The level of activation (A) associated with the recruitment of MNs and their firing depends on the difference between the muscle's actual length (x) and λ, and (during movement) on the rate of change of muscle length (*dx/dt*). Muscle activation increases with the rate of muscle lengthening and decreases with the rate of muscle shortening. Thus, muscle activation is:

$$A = \begin{cases} x - \lambda + \mu \cdot dx/dt & \text{if } x > \lambda - \mu \cdot dx/dt, \\ 0 & \text{if } x \leq \lambda - \mu \cdot dx/dt, \end{cases} \quad (1)$$

where μ specifies the level of reflex damping due to afferent feedback. This parameter may be under central control via γ dynamic MNs. Changes in the control variable λ can be produced by descending inputs to α MNs directly and to γ static MNs.

The model assumes a linear relationship between the muscle's actual length (x) and joint angle (θ): $x = h\theta + b$, where b is a constant length and h is the muscle moment arm. This relationship also specifies the transformation between threshold length for MN recruitment (λ) and the corresponding threshold angle ($\underline{\lambda}$). The angular measure for muscle activation ($\underline{A}$) is obtained by substituting the linear variables in Equation 1 for the corresponding angular ones.

Aspects of the λ model at the single-joint level are presented in Figure 1. A simple single-joint system with a flexor and an extensor muscle is shown in panel D. The joint angle θ is defined such that it increases with extension. Panel A shows the torque-angle curves or ICs for both the flexor and extensor muscles. The system is in static equilibrium when the torque produced by the flexor is equal and opposite to the torque produced by the extensor and there is no external torque. The equilibrium joint angle (R) is specified by the combined actions of both muscles and corresponds to the angle at which the net joint torque is zero. The positions of the flexor and extensor ICs are associated with $\underline{\lambda}_f$ and $\underline{\lambda}_e$, respectively. Consider the effects of briefly perturbing this system. If the arm is perturbed into extension, then both muscle activity and the torques produced by the flexor and extensor muscles will increase and decrease, respectively. The resulting net flexion torque will restore the system's equilibrium. Likewise, if the arm is briefly perturbed into flexion, an extensor torque will restore equilibrium.

With reference to Figure 1, consider two central commands that control the λs of antagonist muscle pairs as a single unit (Feldman, 1980). The central R command governs the EP of the joint by shifting $\underline{\lambda}_f$ and $\underline{\lambda}_e$ in the same direction such that the level of cocontraction is unchanged (compare panels A and B). The central C command specifies the angular range in which both the flexor and extensor muscles are tonically active. This command is produced by shifting $\underline{\lambda}_f$ and $\underline{\lambda}_e$ in opposite directions such that the joint

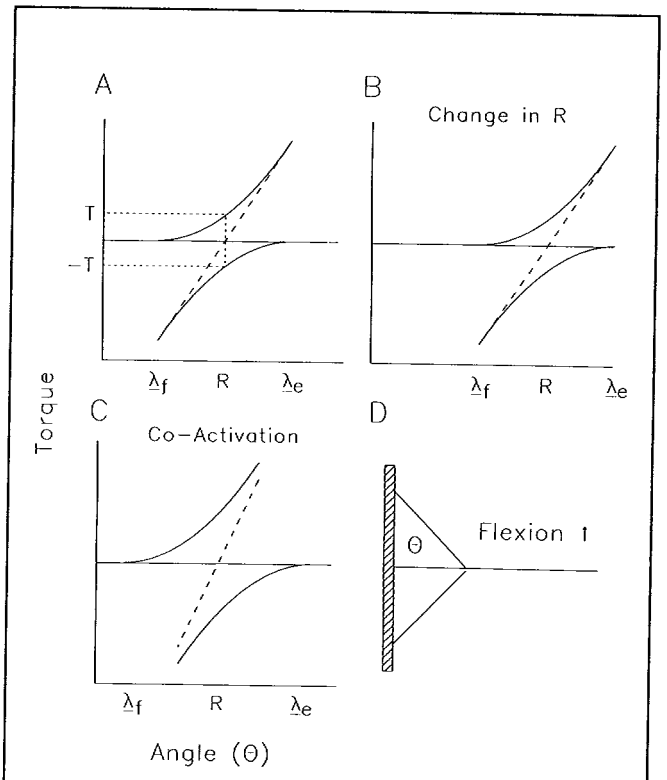

FIGURE 1. Central commands for single-joint control. Antagonist torque-angle curves define the joint equilibrium angle (panel A). The R command governs the EP of the joint (R) by shifting the λs in the same direction (panels A and B). The C command governs the level of cocontraction by shifting the λs in opposite directions (panels A and C).

remains motionless but the level of cocontraction changes (compare panels A and C). Thus, these central commands control the EP of the joint and the level of cocontraction independently. Both the R and C commands produce simultaneous changes in the λs, but they do so in different ways. This figure also illustrates that the C command influences joint stiffness. The sum of the antagonist torque-angle curves (or ICs) represents the net torque-angle curve for the joint (dashed lines) associated with muscle mechanical properties and afferent feedback. As the level of coactivation is increased, the slope of the joint torque-angle curve will increase (compare panels A and C). The slope of this relationship represents the stiffness about the joint. Thus, joint stiffness can be controlled independently of joint angle.

The C and R commands may be defined in terms of joint angle thresholds for MN recruitment as follows (Adamovich & Feldman, 1984):

$$C = (\underline{\lambda}_e - \underline{\lambda}_f)/2. \qquad R = (\underline{\lambda}_e + \underline{\lambda}_f)/2. \quad (2)$$

This definition yields simple expressions for the threshold angles for MN recruitment: $\underline{\lambda}_e = R + C$, and

$\lambda_f = R - C$. For a complete description of the basic mechanisms underlying the λ model, see Feldman (1980, 1986).

In work with the one-joint λ model, central commands have been assumed to vary over time in a simple fashion. The EP (R) has been shifted at a constant rate from the start position to the final position; C has been increased at the start of movement and then gradually decreased after the movement. With this simple form of EP shift, the model is nevertheless able to produce the kinematic and electromyographic patterns observed in single-joint movements.

Two-Joint Control

In the two-joint λ model, as in the single-joint model, central commands control the EP and level of cocontraction independently. In the two-joint model, we assume that the direction of EP shift is specified at the hand level such that the EP of the hand shifts in a straight line toward the target. The rate of shift may also be specified at the hand level. In this article, however, we explore instances in which the rate may be determined at the joint level. In either case, the rate of shift is assumed to be constant. Thus, the nervous system need specify only the direction, rate, and duration of shift of the EP. This control scheme is extended in a direct way to account for trajectory modifications in response to displaced targets. In response to a change in target location, the direction of shift of the hand EP is modified such that it moves toward the new target.

Other equilibrium-point models have been proposed. One of these, the α model of Bizzi and colleagues (e.g., Bizzi, Accornero, Chapple, & Hogan, 1984) differs from the λ model in terms of the basic physiological mechanism proposed to underlie EP shifts. The α model suggests that EP shifts result from direct control of muscle activity. Problems with this model have been discussed elsewhere (Feldman, 1986) and are not considered here.

Flash (1987) has proposed an EP model of two-joint planar arm movement that focuses on the form of the EP shift (i.e., equilibrium trajectory) rather than the mechanism underlying shifts. Flash has shown that if the trajectory of the hand EP is assumed to minimize jerk (such that it has a bell-shaped speed profile and a straight-line path), then predicted hand trajectories are in good agreement with empirical hand trajectories. In Flash's model, as in the two-joint λ model, it is assumed that reaching is planned in terms of the EP of the hand.

In natural reaching, trajectory modifications may be required to correct for initial movement errors or to adjust to moving objects. Displaced or double-step targets have been used previously to examine the on-line control of visually guided arm movements in humans (Gielen, Van den Heuvel, & Denier van der Gon, 1984; Massey, Caminiti, Schwartz, & Georgopoulos, 1986; Megaw, 1974; Paulignan, MacKenzie, Marteniuk, & Jeannerod, 1991; Péllison, Prablanc, Goodale, & Jeannerod, 1986; Soechting & Lacquaniti, 1983; Van Sonderen, Gielen, & Denier van der Gon, 1989) and in monkeys (Georgopoulos, Kalaska, & Massey, 1981).

Models of trajectory modifications have been proposed by Flash and Henis (1991) and Van Sonderen and Denier van der Gon (1990). According to the Van Sonderen and Denier van der Gon model, when a target is displaced, an internal target shifts gradually from the initial target to the displaced target. This, they suggested, may account for the empirically observed graded changes in the direction of hand motion. Flash and Henis (1991) have proposed that movements to displaced targets may involve superposition of two trajectory plans: one from the start to the first target and another from the first to the second target. Thus, these workers suggested that the plans may be carried out in parallel. These two models will be contrasted with the present model in the Discussion.

In this article, we examine horizontal reaching movements to single- and double-step targets. Movements were performed either as fast as possible or at the subject's preferred rate. The focus was on movements directed outwardly from the body. The kinematics of these movements were compared with simulated kinematics generated with the two-joint λ model. The aim was to show that the model can account for the major qualitative features of these kinematics.

The Model

Here we describe a two-joint planar arm model based on the λ model (see also Feldman, Adamovich, Ostry, & Flanagan, 1990; Flanagan, Feldman, & Ostry, 1992). The modeled arm has three pairs of antagonist muscles: pairs of single-joint muscles at the shoulder and elbow and a pair of two-joint muscles. For simplicity, muscle moment arms were assumed to be constant. Geometric and inertial parameters of the model are shown in Table 1 (see An, Hui, Morrey, Linscheid, & Chao, 1981; Winter, 1976). In the equations and figures that follow, vectors are shown in bold-

TABLE 1
Biomechanical Constant Parameters

Segment	Mass (kg)	Moment of inertia (kg m²)	Length (m)	D[a] (m)
Upper arm	1.0	.065	.3	.13
Lower arm	1.2	.1	.4	.17

Muscle pair	Shoulder moment arm (m)	Elbow moment arm (m)	α (rad⁻¹)	ρ (N)
Shoulder	.03		1.14	4.4
Elbow		.03	1.14	2.2
Double	.01	.03	1.14	2.2

[a]Distance from proximal end to the center of mass.

faced type. The same symbols, without bold-face, are used to denote the magnitude (length) of the vectors.

Control Signals

In the two-joint model, movements are produced by the central command, **U**, which specifies the direction and rate of shift of the hand EP. The corresponding angular equilibrium velocities (EVs) at the shoulder ($d\mathrm{R}_1/dt$) and the elbow ($d\mathrm{R}_2/dt$) are then computed based on the arm geometry. Simultaneously, C commands specify coactivation zones for the three antagonist muscle pairs. The appropriate R and C commands are used to obtain values of λs for each muscle. These control signals, in combination with the current values of kinematic variables, are used to compute muscle activations and muscle torques, as described above for single-joint control. The latter are substituted in Newton-Euler's equations of motion, which are integrated to obtain the resulting movement. Movement corrections in response to target displacements are produced by changes in the direction or magnitude of **U**. We also have considered a modification to this control scheme whereby the rate of EP shift is specified at the joint level.

Figure 2 shows the hand equilibrium velocity vector, **U**. The direction of **U** is defined by the angle, β, between **U** and the *x*-axis. The relative direction of **U** is defined by the angle σ_1 or σ_2 between **U** and the vector ($\mathbf{r}_1$ or $\mathbf{l}_2$ respectively) directed from the center of the joint to the end point. The equilibrium arm configuration is specified by the current values of commands R_1 and R_2. These commands can also be represented by vectors that are directed along the axes of rotation of the joints. Vector shift **U** is associated with the rotational commands for the joints and, consequently, the following vector equation is valid:

$$\mathbf{U} = \mathbf{r}_1 \times d\mathbf{R}_1/dt + \mathbf{l}_2 \times d\mathbf{R}_2/dt, \quad (3)$$

where the right-hand side represents the sum of two vector products. Each of the vector products defines the shift of the arm end point due to rotation in one joint when the other joint is motionless. The shifts associated with changes in $\mathbf{R}_1$ and $\mathbf{R}_2$ are perpendicular to the corresponding radial vectors $\mathbf{r}_1$ and $\mathbf{l}_2$. To solve this equation for joint EVs, we take projections of **U** and its components in the right-hand side to lines parallel first to $\mathbf{r}_1$ and then to $\mathbf{l}_2$. As a result, we get the following scalar equations:

$$d\mathrm{R}_1/dt = \mathrm{U}\cos\sigma_2 / \mathrm{r}_1 \sin(\sigma_2 - \sigma_1), \quad (4)$$

$$d\mathrm{R}_2/dt = \mathrm{U}\cos\sigma_1 / \mathrm{l}_2 \sin(\sigma_1 - \sigma_2),$$

where $\sigma_2 = \mathrm{R}_1 + \mathrm{R}_2 - \beta$, $\tan(\sigma_1) = [\mathrm{l}_2\cdot\sin(\sigma_2) - \mathrm{l}_1\cdot\sin(\beta - \mathrm{R}_1)]/[\mathrm{l}_1\cdot\cos(\beta - \mathrm{R}_1) + \mathrm{l}_2\cdot\cos(\sigma_2)]$ and $\mathrm{r}_1 = \mathrm{l}_1\cdot\cos(\beta - \mathrm{R}_1 + \sigma_1) + \mathrm{l}_2\cdot\cos(\sigma_2 - \sigma_1)$. Note that the geometric relationships described here refer to equilibrium states of the limb that allow us to replace θ_i by R_i.

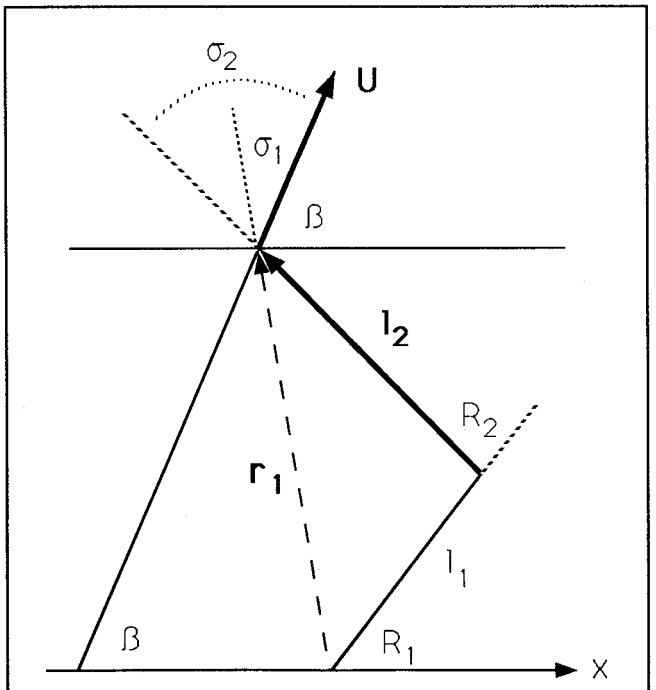

FIGURE 2. Geometry used to calculate the EVs at the shoulder ($d\mathrm{R}_1/dt$) associated with the EV of the hand (**U**).

Intermuscular Coordination

Control variables for double-joint muscles are coordinated with those for single-joint muscles in a specific way. Note that the length of a two-joint muscle (x_d) depends on both the shoulder angle (θ_1) and the elbow angle (θ_2):

$$\mathrm{x}_d = \mathrm{h}_1\cdot\theta_1 + \mathrm{h}_2\cdot\theta_2 + \mathrm{b}_d, \quad (5)$$

where h_1 and h_2 are the two-joint muscle moment arms at the shoulder and elbow, respectively, and b_d is a constant. A generalized joint angle (θ_d) may be defined as follows:

$$\theta_d = (\mathrm{x}_d - \mathrm{b}_d) / (\mathrm{h}_1 + \mathrm{h}_2). \quad (6)$$

Equation 4 can be used to transform the threshold length λ_d into a generalized threshold angle ($\underline{\lambda}_d$) to specify R and C commands for double-joint muscles in a way similar to that for single-joint muscles. Note that θ_d defines a family of postures subject to the kinematic constraint in Equation 5. Likewise, $\underline{\lambda}_d$ defines a family of equilibrium postures at which the threshold for MN recruitment is reached.

In the model, the R command for the pair of two-joint muscles (R_3) is related to those of the single-joint muscles (R_1 and R_2) according to the following equation:

$$\mathrm{R}_3 = (\mathrm{h}_1\cdot\mathrm{R}_1 + \mathrm{h}_2\cdot\mathrm{R}_2)/(\mathrm{h}_1 + \mathrm{h}_2). \quad (7)$$

To clarify this rule, let the coactivation command C be zero for all muscles. For any given limb configuration, in the absence of an external load, $\theta_1 = \mathrm{R}_1$, and $\theta_2 = \mathrm{R}_2$, that is, the threshold lengths of all single-joint muscles coincide with their actual lengths. Equation 7 means that the double-joint muscles reach their activation thresholds at the same arm configuration. In other words, the anatomical relationships between actual lengths of all arm muscles are mir-

rored in the control signals (the principle of biomechanical correspondence).

In some simulations, an upper limit was imposed on the joint equilibrium velocities (EVs). If one of the joint EVs reached this limit, the other was restricted to preserve the ratio of joint equilibrium velocities and, hence, the direction of the shift in the EP of the hand. This method exploits the fact that, for any given hand position, there is a unique relationship between the direction of hand movement and the ratio of joint velocities (see Equation 3). Because this relationship depends on the position of the limb, when the equilibrium velocity of one joint is limited, the extent to which the other is restricted will depend on the limb's position.

Muscle Torques

The generation of muscle torques in the model is described by the following set of equations:

$$T = \rho \cdot h \cdot (e^{\alpha \cdot \underline{A}} - 1). \quad (8)$$

$$M + \tau_1 \cdot dM/dt + \tau_2^2 \cdot d^2M/dt^2 = T. \quad (9)$$

$$n = M \cdot (1 + a \cdot d\theta/dt). \quad (10)$$

Equation 8 specifies the steady-state value of isometric muscle torque T as a function of the level of muscle activation (A). The muscle moment arm, h, and the coefficients ρ and α are given in Table 1. The constant ρ is related to the strength of the muscle, and the constant α is a form parameter. In statics, the form of this equation approximates the *invariant characteristic* (IC), which represents the torque-angle properties of the muscle plus afferent feedback (Feldman, 1966). In general, according to Equations 1 and 8, muscle activity and muscle torque are velocity dependent.

Equation 9 accounts for the fact that force, and hence the torque, generated by the muscle rises and falls gradually as the level of muscle activation changes because of the calcium-dependent process of excitation-contraction coupling. According to Equation 9, the current value of isometric muscle torque (M) gradually reaches the steady-state value T. This process was simulated using a second-order low-pass filter of variable T with time constants $\tau_1 = .02$ s and $\tau_2 = .01$ s.

The force generated by the muscle depends on the rate of sliding of muscle filaments, as described by Hill's (1938) force–velocity relationship. Equation 10 for current muscle torque (n) is a linearized version of this relationship. The equation is given for a muscle whose length increases with joint angle θ. The value of time constant a is .03 s. Note that both reflex damping, μ (see Equation 1), and the intrinsic muscle component of damping, a, were represented in the model.

The torques at each joint are the sum of the single- and double-joint muscle torques. In the simulations, joint accelerations at the shoulder and elbow were derived from joint torques by using Newton-Euler's equations of motion for the two-joint planar arm (see Hollerbach & Flash, 1982; Soechting & Lacquaniti 1981) with inertial and geometrical constants in Table 1.

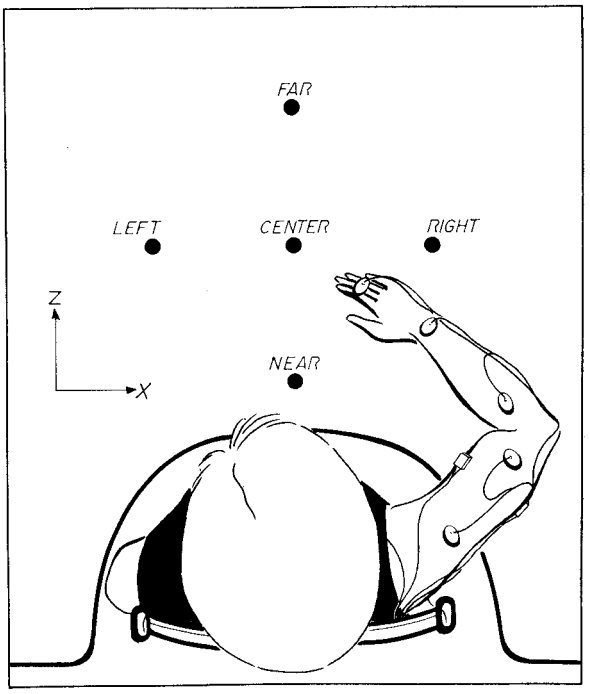

FIGURE 3. Top view of a subject sitting at the experimental table. The positions of the five target LEDs are shown. Five markers used to record the trajectories of the hand and arm can also be seen.

Methods

Subjects and Apparatus

Four subjects performed horizontal pointing movements to light-emitting diodes (LEDs). A top view schematic of the table with a seated subject is shown in Figure 3. The positions of five target LEDs and the *x*- and *z*-axes are shown. The distance from the center LED to the four peripheral targets was 23 cm, and the distance from the near target to the subject was 8 cm. The subjects were positioned such that they could move their arms freely in a horizontal plane approximately 3 cm above the table surface. The forearm was fully pronated. Subjects were able to move their arms horizontally with little deviation in the vertical. This indicates that they did not rotate their upper arm. Because these movements were unrestrained, however, there may have been small measurement errors associated with nonplanar arm motion.

Data Recording and Processing

The positions of infrared-emitting diodes (IREDs) attached to the subject (see Figure 3) were recorded three dimensionally (3-D) with the Watsmart™ system. IRED

positions were sampled at 400 Hz and digitally low-passed at 10 Hz, using a fourth-order, zero-phase-lag Butterworth filter. The elbow angle calculation was based on the scalar product between the 3-D vector joining the IREDs on the lower arm of the 3-D vector joining the IREDs on the upper arm. The shoulder angle calculation was based on the scalar product between the latter 3-D vector and the z-axis.

Experimental Procedure

Single-step trials were initiated from either the near or center target and were directed toward one of the four remaining targets. Double-step trials were initiated from the near target. These were initially directed toward the center LED and then to left, right, or far LEDs. The timing and position of targets were randomly varied. Movements were performed either as fast as possible or at the subject's preferred rate. Ten trials were collected in each condition.

In fast double-step trials, interstimulus intervals (ISIs) ranged from 10 to 400 ms; and in preferred-rate double-step trials, ISIs ranged from 30 to 500 ms. The study included trials with very short ISIs ($\leq$ 60 ms), in which the target was displaced prior to movement onset; trials with longer ISIs, in which the target was displaced while the hand was moving to the initial target; and trials with very long ISIs ($\geq$ 250 ms), in which the hand reached the initial target before the target was displaced.

Instructions

Fast and preferred-rate movements were recorded in different experimental sessions. In the fast movement condition, subjects were asked to move as soon and as quickly as possible. In the preferred-rate condition, subjects were instructed to move as soon as possible but at a comfortable speed. Subjects were asked to move to the currently illuminated target. At no time was more than one target presented. In sets of trials in which only single-step targets were included, subjects were informed of this in advance.

Subjects were instructed to move their hands in a horizontal plane just above the table. In addition, they were asked not to make corrective adjustments as they approached the target. Thus, a high degree of spatial accuracy was not demanded. No restraining devices were placed on the arm. However, subjects were instructed not to move their wrists during the movement. We observed that subjects were able to comply with these instructions.

Single-step trials starting from the near LED and directed to the center target were denoted *near→center* trials. Double-step trials, starting from the near LED, in which the far target was presented after the center target, were denoted as *near→center→far* trials.

Results

We examine trajectories to single-step targets and then consider responses to double-step targets. Our approach is to present actual and simulated paths and velocity profiles together. In addition, examples of central control signals used in simulations are presented. However, we will first consider the selection of parameters used in the simulations.

Simulation Parameters

Although the model has many parameters, most of these are constants that reflect geometric and mechanical properties of the arm (see Table 1). The only parameters that were varied in the simulations are those related to central control signals. These are: the rate, direction, and timing of hand EP shift, the amplitude of the C commands for each muscle pair, and the damping coefficient μ. (The magnitudes of the U, C, and μ parameters used in simulations are given in Table 2.)

The direction of EP shift was always toward the target. Thus, in effect, this parameter was not varied. The damping coefficient μ was the same in all simulations (although in a small number of cases μ was increased at the very end of the movement to reduce terminal oscillations). Finally, the C commands for the single-joint elbow muscles and the double-joint muscles were always the same. Thus, the only parameters that were varied across simulations were the rate and timing of EP shift, the C commands for the single-joint shoulder muscles, and the C commands for the single-joint elbow muscles and double-joint muscles. The rates of EP shift and magnitudes of C used here were within the range of values established in previous work on single-joint motions (e.g., Abdusamatov, Adamovich, & Feldman, 1987). Exact values were selected to give good qualitative fit between the simulated and actual trajectories.

The effects of varying these parameter values on simulated trajectories are assessed below. We emphasize that the goal of this modeling exercise was to provide evidence that the model can reproduce qualitative features of the movement trajectories. The aim was not to obtain precise values

TABLE 2
Central Control Parameters for Single- and Double-Step Movements

Parameter	U (m/s)	C elbow and double (rad)	C shoulder (rad)	μ (s)
		Single-step		
Near→center	4	1	1.5–2	.075
Near→far	4	1	2	.075
Near→left	4	1	2	.075
Near→right	4	1	2	.075
Center→far	2.2	1	2	.075
		Near→center→right		
ISI 20	4 / 4	1	1	.075[a]
ISI 60	4 / 2.2	1	1	.075[a]

[a]μ was increased to .15 toward the very end of the movement.

for parameters, as the model has obvious simplifications. We wanted to show that the model can account for the direction and the extent of hand path curvature and the overall shape of the velocity profiles. The extent to which that model was successful in this regard was evaluated by comparing simulated and actual movement trajectories.

Single-Step Targets

Horizontal plane hand paths of fast movements to single-step targets initiated from the near LED are shown in Figure 4 for all four subjects (bottom panels). Dotted lines represent paths to the far target. A left-to-right curvature (with respect to the direction of motion) in the hand paths was observed for motions to the center and far targets and especially the right target. A slight left-to-right curve was also evident in the paths directed to the left target for two of the subjects (A and C). Many of the paths were sharply curved toward the end of the motion. For example, the hand paths to the left target hooked to the left at the end of the movement. For three of the subjects, the motion paths to the center and far targets diverged near to the start position.

Corresponding simulated hand paths are presented in the top right panel of Figure 4. In these simulations, the hand EP was shifted in a straight line toward the target. These

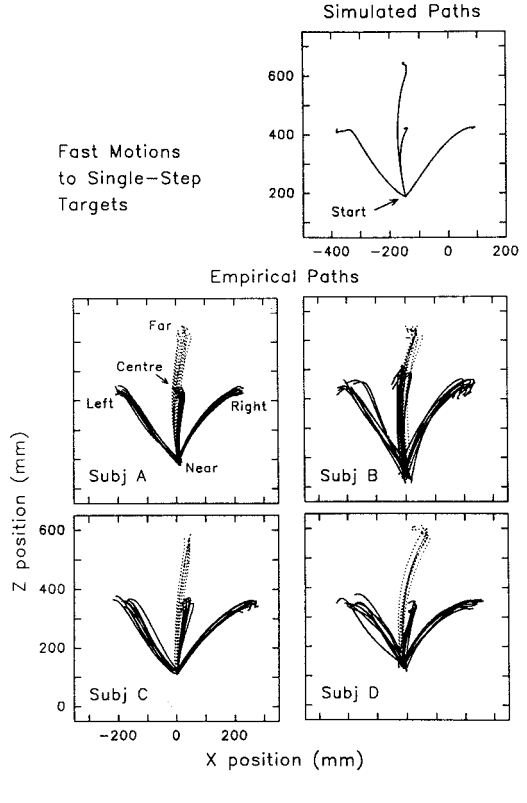

FIGURE 4. Simulated (top right panel) and empirical hand paths for four subjects (bottom panels). In these simulations, the hand EP was shifted in a straight line toward the target at a rate of 4 m/s. The curvature of the simulated and empirical paths are similar.

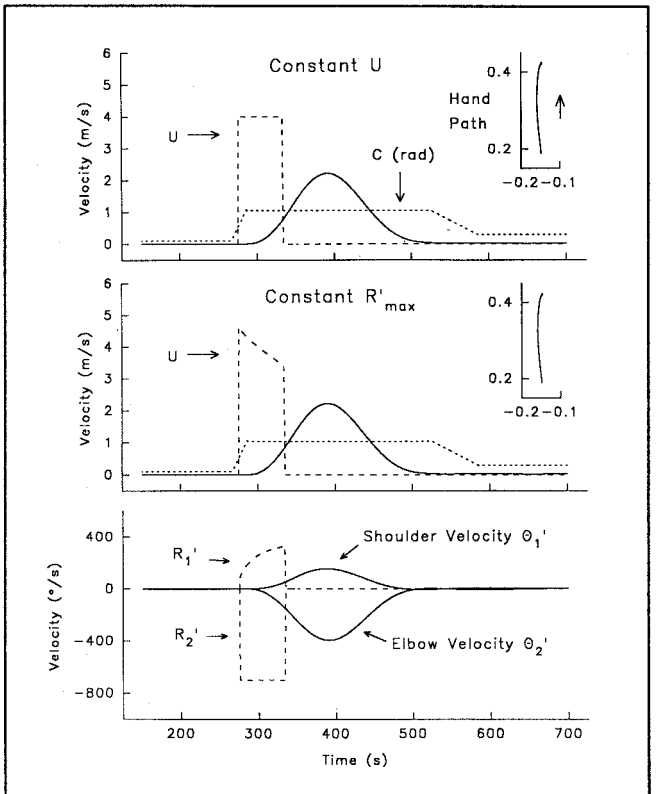

FIGURE 5. Simulated central commands and kinematics for near→center motions. In the simulation shown in the top panel, the hand EV (U) was constant at 4 m/s. In the simulation shown in the bottom two panels, the joint EVs (lower panel, dashed) were limited to ± 700°/s. In both simulations, the form of the hand speed profile (top two panels, solid) and hand path were similar to those observed empirically. The vertical axis also represents the amplitude of the C command in radians.

simulated paths were characterized by the same left-to-right curvature as the empirical paths and exhibited similar hooks at the end of the motion. In the model, the final EP was reached well before the end of the movement. (For example, with a rate of hand EP shift of 4 m/s, it takes 50 or 100 ms to shift .2 or .4 m, respectively.) The hooks in the simulations occurred because the hand overshot the final stationary EP. This suggests that the hooks observed empirically may result from movement dynamics and not planned corrective movements. Although the hand EP was shifted in the same direction for motions to the center and far targets, the simulated hand paths diverged at about half the distance to the center target. A similar divergence was observed empirically for three of four subjects.

In Figure 5, simulated central commands and kinematics for a fast response involving the near→center target are shown. Consider first the top panel, in which the rate of shift of the hand EP (U) was constant. The magnitude of the C command for the shoulder muscles was 1.5 times the C commands for elbow and double-joint muscles (dotted). However, the form of the C command was the same for all

three muscle pairs; C increased just before movement onset, was constant during the movement, and then decreased gradually after the end of the movement. With these simple control signals the model was able to generate smooth hand speed profiles (solid) and curved hand paths like those observed empirically.

Examination of movements in different regions of the work space (see below) has led us to consider the possibility that the rate of EP shift may be determined, in some cases, at the joint level. In the simulation shown in the middle and bottom panels of Figure 5, the maximum joint EV was set at 700°/s. This is around the maximum EV that has been estimated for fast, one-joint elbow motions (Abdusamatov et al., 1987). The equilibrium and predicted velocities of the shoulder and elbow joints are shown in the bottom panel. As can be seen, the elbow EV (R_2') was 700°/s throughout the EP shift. The shoulder EV (R_1') varies to preserve the direction of shift of the hand EP. Because the mapping between joint velocities and hand velocity depends on the position of the arm, the rate of shift of the hand EP (middle panel) changes over the movement when the elbow EV is held constant.

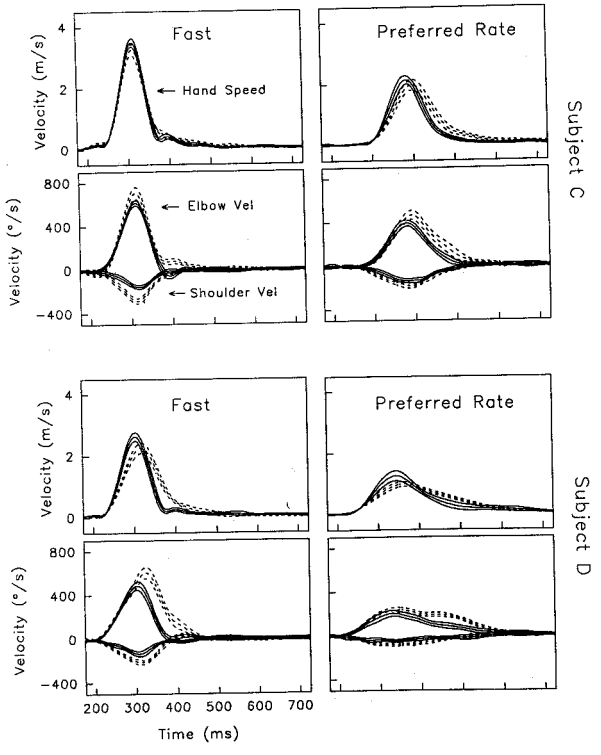

FIGURE 6. Hand and joint velocity profiles for fast (left) and preferred-rate (right) near→center (solid) and center→far (dashed) motions. Mean and ± one standard deviation curives are shown. Although the peak hand velocities tended to be smaller for the center→far motions, the joint velocities were greater.

Motions in Different Regions of the Work Space

Because of the geometry of the multijoint arm, movements carried out in different regions of the work space that are equal in hand movement amplitude may have different amplitudes of joint motion and vice versa. Thus, movements of equal hand speed in different regions of the work space may have considerably different joint angular velocities. The question arises as to whether movement rate may be coupled to hand amplitude or joint amplitude.

In Figure 6, hand speed profiles and corresponding joint angular velocity profiles of fast and preferred-rate movements are shown for Subjects C and D. Velocities of near→center (solid traces) and center→far (dotted traces) movements are shown. In each panel, the averaged velocity profile (based on 8 to 10 trials) and the profiles corresponding to ± one standard deviation are shown. The averaged velocity profiles have been aligned with respect to movement onset (i.e., the point at which the hand speed reached .2 m/s).

The near→center and center→far movements shown in Figure 6 were similar in terms of hand movement direction and amplitude. However, the amplitudes of joint rotation at both the shoulder and elbow were greater in the center→far movement. The data from the two subjects shown in the figure typify the two patterns of results that we observed. The duration and the form of the hand speed profiles of Subject C's fast movements were similar, whereas the initial slopes of the joint velocity profiles were steeper in the center→far movement. In all other cases, the duration of the center→far movement was greater and the initial slope of the hand speed profile of this movement was smaller. In addition, the initial slopes of the joint velocity profiles tended to be similar for the two movements. These data suggest that hand speed depends on the region of the work space in which the movement is produced.

Figure 7 demonstrates that the rate of shift of the hand EP may be modified for movements in different regions of the work space to adjust for the position-dependent mapping between hand and joint velocities. The figure shows consecutive (simulated) near→center and center→far motions. The top panel illustrates the rate of shift of the hand EP (U) and the predicted hand speed profile under two conditions. In one condition, the hand EP shifted at a constant rate of 4 m/s for both movements (dashed). In the other condition, the rate of shift of the hand EP was reduced to 2.2 m/s for the second movement (dashed-dotted). The middle panel shows the joint EVs (dashed) and predicted joint velocities (solid) corresponding to the case in which the hand EP shifted at 4 m/s for both movements. The bottom panel shows the joint EVs and predicted joint velocities corresponding to the condition in which the rate of shift of the hand EP was reduced to 2.2 m/s for the second movement. As illustrated in the top panel, the peak hand speed of the second motion generated with a hand EP shift of 4 m/s (solid) was greater than that produced with a hand EP shift of 2.2 m/s (long dashed).

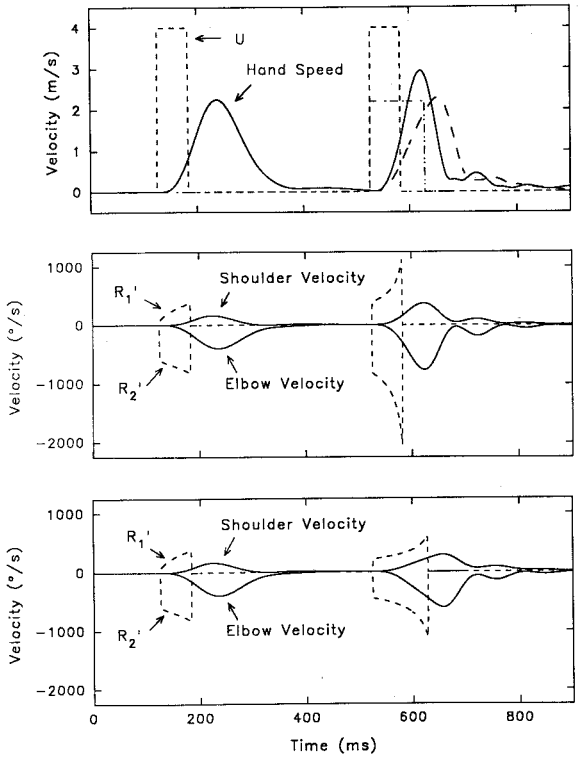

FIGURE 7. Simulated near→center and center→far motions. The top panel shows rates of hand EP shift (U) and predicted hand speed profiles. In one case, U was 4 m/s for both movements, and in the other, U was reduced to 2.2 m/s for the center→far motion. Joint EVs and predicted velocities corresponding to these two cases are shown in the middle and bottom panels.

When the rate of shift of the hand EP was 4 m/s, the joint EVs were far greater in the second movement and the elbow EV exceeded −1500°/s (middle panel). As a result, the peaks and initial slopes of the predicted joint and hand velocity profiles were clearly greater for the second movement, unlike the actual data (see Figure 6). Moreover, the elbow EV of −1500°/s was more than twice the EV estimated by Abdusamatov et al. (1987) for fast, single-joint elbow motions (500 to 700°/s). However, kinematic patterns similar to those observed empirically can be obtained by simply reducing the rate of shift of the hand EP for the second movement. This suggests that the rate of hand EP shift may vary depending on the region of the work space.

An alternative scheme that might be used to deal with the position-dependent relation between hand and joint velocities is illustrated in Figure 8. This figure shows simulated near→center and center→far motions in which the maximum joint EV was ±700°/s. In this particular case, the elbow EV reached −700°/s while the shoulder EV varied so as to preserve the direction of shift of the hand EP (bottom panel). As shown in the top panel, the effect of specifying a maximum joint EV was to reduce the overall rate of shift of the hand EP during the second, distal movement. The predicted hand speed profiles of the first and second movements were similar to those obtained with constant rate shifts of the hand EP where the rate was reduced for the second movement (see Figure 7).

Responses to Double-Step Targets

Movements to double-step targets are typically characterized by bimodal hand speed profiles. Flash and Henis (1991) have suggested that these bimodal profiles reflect the summation of submovements that overlap in time. In Figure 9, we illustrate that a bimodal hand speed profile can also be generated by consecutive EP shifts that are separated in time. The figure shows a near→center→far motion produced by the model. The top panel shows the rate of shift of the hand EP (dotted), the predicted hand speed profile (dashed), and the C command for the elbow muscles (solid). The EV of the elbow was limited to ±700°/s. The EP shifted first to the center target and then to the far target. The time interval between the initiation of the two EP shifts, or ISI, was 120 ms. Note that the EP reached the first target in 60 ms. The second EP shift began 60 ms later.

In the bottom panel, the hand speed profile generated by the model (dashed) is compared with the profile (solid) generated by superimposing two minimum-jerk velocity profiles (dotted). The first minimum-jerk profile was aligned with the initial part of the simulated profile and was subtracted from it. The second minimum-jerk profile was then aligned with the remainder of the simulated pro-

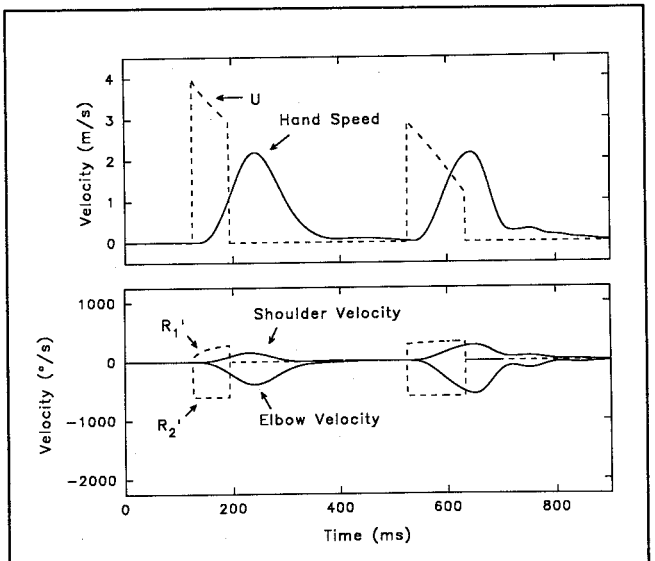

FIGURE 8. Effect of limiting the rate of joint equilibrium shift. Simulated near→center and center→far motions in which rate of EP shift was controlled at the joint level. The EV of the elbow was constant, and the shoulder EV was adjusted such that the hand EP shifted in a straight line toward the target.

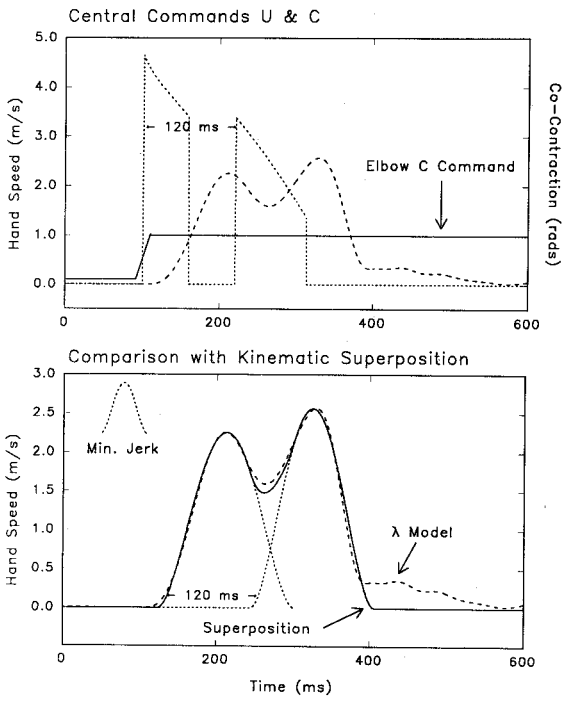

FIGURE 9. Simulated velocity profiles. Top: Central commands and predicted hand speed profile for a simulated motion to the near→center→far target. Bottom: Comparison of the λ model with superimposed minimum-jerk trajectories.

file. This procedure is similar to those used by Flash and Henis (1991) and Milner (1992). The onset times of the two minimum-jerk velocity profiles were 120 ms apart as were the two EP shifts in the simulated motion. Thus, the kinematic superposition technique, based on minimum-jerk trajectories, and the two-joint planar arm model, based on the EP hypothesis, appear to make similar predictions about the timing of the two responses in double-step trials.

In Figure 10, empirical hand paths for near→center→left (dotted lines) and near→center→right (solid lines) targets are shown for Subjects A and C. The solid horizontal bars mark the points at which the paths to the left and right final targets diverged. At both fast (top) and preferred (bottom) rates, the hand paths to the left and right targets diverged progressively later as the ISI increased. Similar patterns were observed for all subjects.

Figure 11 shows empirical and simulated hand paths and speed profiles for fast, double-step responses to near→center→right targets with ISIs of 20 (short dashes) and 60 (dots) ms and fast, single-step responses to the near→center (dashes) and near→right (solid) targets. In these simulations, the rate of EP shift was specified at the hand level. However, a limit of ± 700°/s was imposed on joint EVs. This accounts for the slight reductions in U seen at the end of the shift to the center target (panel B) and at the onset of the EP shift to the right target (panel E). In these simulations, the level of reflex damping (μ) increased from .075 to .15 s^{-1} at the end of the movement to reduce terminal overshoots.

In the model, the ISI refers to the time interval between the first and second EP shifts. With the 20-ms ISI (panel D), the hand EP started to shift toward the second (right) target well before it reached the first (center) target. However, with the 60-ms ISI (panel C), the hand EP started to shift toward the second target at about the same time that it reached the first target. In this case, it was necessary to decrease the rate of shift of the hand EP (from 4 to 2.2 m/s) to the second target. Recall that the rate was also 2.2 m/s for the simulated center→far movement shown in Figure 7.

The hand paths and speed profiles generated by the model were qualitatively similar to the empirical paths and profiles. For example, the model was able to predict the unimodal and bimodal hand speed profiles of the double-step trials with ISIs of 20 and 60 ms, respectively. The model was also able to predict the points of divergence of the hand paths for motions with different ISIs.

Sensitivity of Kinematics to Changes in Parameter Values

We examined the sensitivity of predicted kinematics to variations of central control parameter values. Figure 12 shows predicted hand paths (left) and hand velocity profiles (right) for movements from the near target to the center target. Similar results were obtained for movements to other targets and from other starting positions. The emphasis of this qualitative analysis of sensitivity to parameter change was to show the stability of predicted kinematics.

The rate of hand EP shift (U), the level of reflex damping (μ), and the amplitudes of the cocontraction commands (C) were varied. In all cases, the ranges of values exceeded those used in the simulations described elsewhere in this article. U was varied from 1.6 to 4 m/s, μ was varied from .1 to .05 s, and Cs for the elbow and double-joint muscle pairs were varied from .6 to 1.2 rad, all in equal steps. (C for shoulder muscles was always one and a half times C for the other muscles). When not varied, U, μ, and C were 3.5 m/s, .075 s, and 1 rad, respectively. These correspond to typical values used in simulations.

The predicted kinematics were stable across changes in parameter values. In many cases, variation of parameter values had a relatively small affect on the kinematics patterns. However, even where clear changes in the kinematics were observed, the basic form was by and large preserved. Several observations regarding the predicted kinematics may be made. Changes in C had very little affect on the trajectory, whereas changes in U produced systematic changes in predicted hand velocity. This effect was greater at lower values of U. Increasing and decreasing μ from the value of .075 s used in the model produced under- and

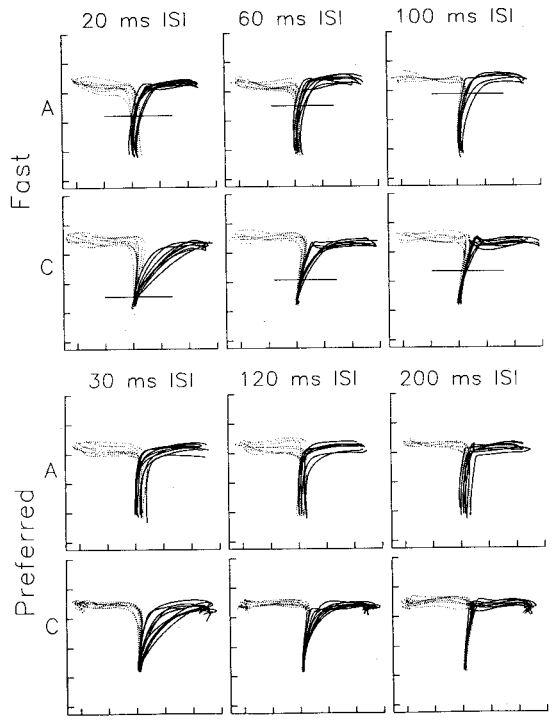

FIGURE 10. Double-step responses. Hand paths to near→center→left (dotted) and near→center→right targets (solid) with different ISIs. The tick interval on both axes is 10 cm.

overdamped movements similar to those that sometimes can be observed empirically.

Discussion

We have provided evidence that a two-joint version of the λ model can account for global kinematic features of horizontal reaching movements to fixed and displaced targets. Four main points may be emphasized. First, the model with simple control signals was able to reproduce key features of hand paths and velocity profiles of movements between different targets. Second, in the model, the rate and direction of EP shift may be controlled at different levels. In horizontal reaching movements, the results suggest that the direction of EP shift is specified at the hand level (see also Flash, 1987), whereas the rate of EP shift may be specified at the hand or joint level. Third, there is some evidence that the movements in different parts of the work space may have different hand EVs. Lastly, the control scheme whereby the hand EP is shifted in a straight line toward the target can account for trajectories to both fixed and displaced targets.

In this article, we have focused on movement kinematics. However, the λ model also predicts muscle activity patterns (Feldman et al., 1990). Comparisons between actual and predicted muscle activity patterns would be of value in testing the model and estimating parameters. Work with the single-joint model has shown that predicted muscle activation patterns are generally more sensitive to parameter changes than are kinematic patterns. For example, changes in the C command clearly affected the level of activity in antagonist muscle pairs in the model, but this had a relatively small affect on kinematics (see Figure 9).

In the model, movements are generated by shifts in the equilibrium arm configuration. Different ways of specifying the rate of EP shift were considered. One possibility is that central commands specify the rate of shift of the hand EP. In this case, the central nervous system (CNS) may simply change the rate of hand EP shift for motions in different regions of the work space. Alternatively, the system may specify a constant EV at one joint and adjust the EV of the other joint to preserve the direction of shift of the hand EP. A third possibility is that the rate of EP shift is initially specified at the hand level but is limited at the joint level if one of the joint EVs reaches a ceiling (e.g., 700°/s). In this third scheme, the rate of shift of the hand EP would be limited only in fast movements. One other possibility is that the system's force-generating mechanism may saturate at high joint EVs so that central control signals need not lower the rate of EP shift.

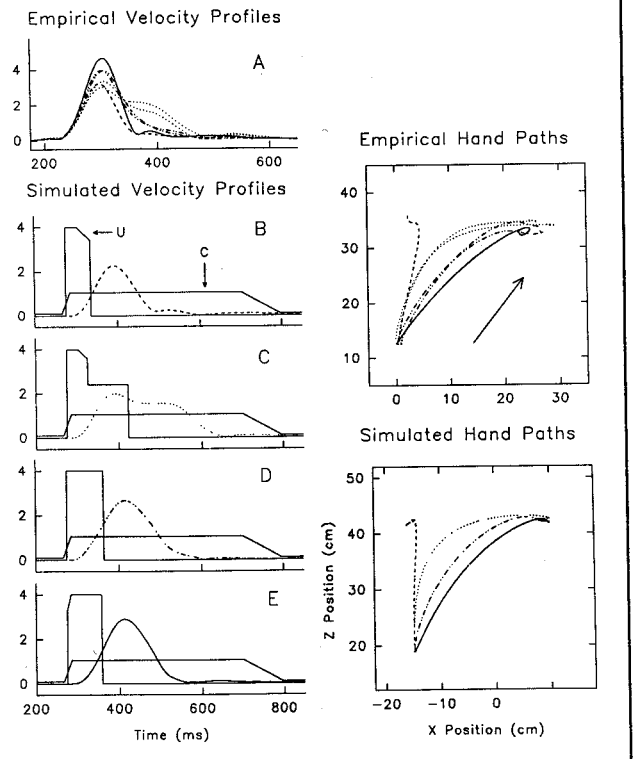

FIGURE 11. Effects of ISI on hand kinematics. Empirical and simulated hand speed profiles for single-step near→center (dashes) and near→right (solid) targets and double-step near→center→right targets with ISIs of 20 (dash-double-dot) and 60 (dotted) ms.

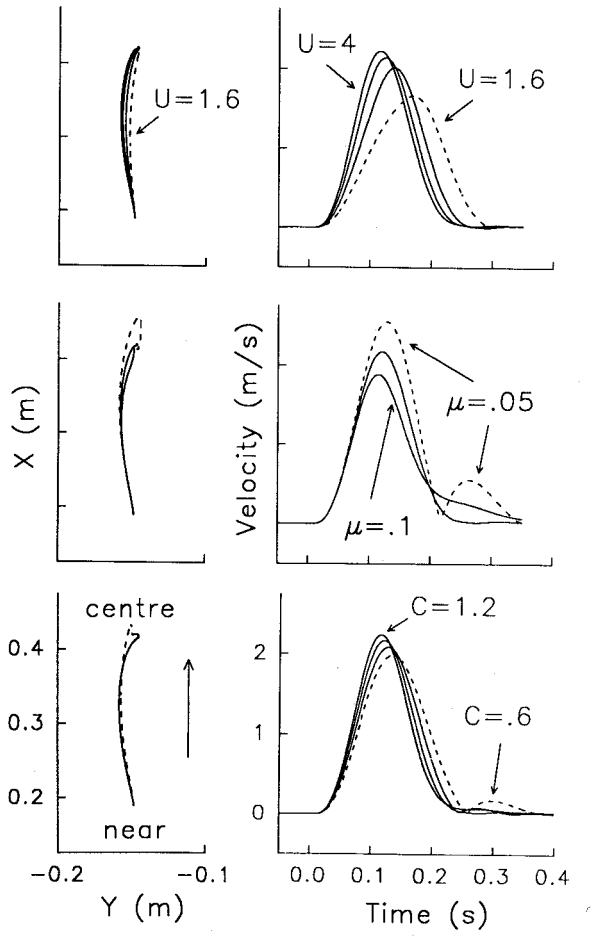

FIGURE 12. Effects of varying central control parameters on simulated kinematics. Sensitivity of predicted kinematic patterns to variation in central control signal parameters. Note, for the C command, paths are shown corresponding to C = 1.2 and C = .6 (dashed).

Specifying both the rate and direction of the EP shift at the hand level has the advantage of simplicity. However, the rate of shift may have to be adjusted for motions in different work space regions to ensure that joint EVs stay within reasonable limits. Alternatively, joint EVs may be specified directly. Nevertheless, the joint EVs must be coordinated to shift the hand EP in the desired direction. Thus, whether the rate of EP shift is specified at the hand or the joint level, the position-dependent relation between hand and joint kinematics must be taken into account.

Regardless of whether the rate of EP shift is specified at the hand or joint level, central commands need only specify the rate, direction, and duration of EP shift. Amplitude is specified by the duration of the EP shift and does not need to be known prior to movement initiation. If the target is displaced early in the trial, the EP may simply continue to shift toward the new target, and thus, as has been observed experimentally (Flanagan et al., 1992; Péllison et al., 1986), there will be no inflection point associated with this correction—as if the movement were programmed to the far target from the beginning. In contrast, Flash (1987) assumed that the velocity profile of the hand EP is bell-shaped and scales with amplitude. Thus, amplitude must be specified prior to movement initiation. In Flash's model, smoothness is considered to be a fundamental principle underlying the planning and production of movement and is directly reflected in the central commands underlying EP shift (see also Hogan, 1984). According to the λ model, movements are smooth because of the system's natural dynamics.

Trajectory Modifications in Response to Displaced Targets

Several differences between the λ model and the model proposed by Van Sonderen and Denier van der Gon (1990) may be highlighted. To account for the gradual changes in actual movement direction following target displacement, Van Sonderen and Denier van der Gon have assumed that an internal target shifts gradually from the initial target to the displaced target. In contrast, the λ model assumes that gradual changes in the direction of movements result from the natural dynamics of system. The mechanism of force generation in the Van Sonderen and Denier van der Gon model is quite different than in the λ model. Movements are initiated by specifying agonist torques that move the hand toward the internal target. Their model assumes that there is an internal hand that shifts toward the target. The role of the internal hand is to trigger antagonist torques. When the internal hand reaches the internal target, antagonist torques are specified so as to break the movement.

In the present model, responses to first and second targets are controlled in the same way, and the nature of the control mechanism does not change during the movement. In contrast, control mechanisms underlying responses to the first and second target differ in the Van Sonderen et al. (1990) model. In particular, whereas the internal target shifts instantaneously to the first target, it shifts gradually toward the second target. Moreover, the control rule whereby the internal hand shifts in a straight line toward the internal target is suspended when the internal hand reaches the shifting internal target in double-step responses.

Flash and Henis (1991) suggested that trajectory modifications in reaching to displaced targets may involve the summation of two trajectory plans. When the target is displaced, the first plan (for moving to the initial target) is continued and the second plan (for moving from the first to the second target) is initiated. These workers suggested that the two movement plans may be carried out in parallel. As pointed out by Flash and Henis, an advantage of this scheme is that the position of the hand does not have to be known to plan the second trajectory.

In this article, we showed that superposition at the level of kinematics does not necessary imply that there is superposition of control signals. We have shown that a scheme

in which the hand EP stops shifting toward the initial target and starts shifting toward the second target after the target is displaced can account for the kinematics of responses to double-step targets. In this scheme, movements to first and second targets are organized consecutively or serially. Note that formally, any shift in the EP can also be represented in terms of two superimposed simultaneous EP shifts. Evidence for these alternatives in the context of central control might be provided by neurophysiological studies.

ACKNOWLEDGMENT

This research was supported by grants from the Natural Sciences and Engineering Council of Canada and the Fond pour la formation de chercheurs et l'aide à la recherche (FCAR) program of Québec.

REFERENCES

Adamovich, S. V., & Feldman, A. G. (1984). Model of central regulation of the parameters of motor trajectories. *Biophysics, 29,* 338–342.

Abdusamatov, R. M., Adamovich, S. V., & Feldman, A. G. (1987). A model for one-joint motor control in man. In G. N. Gantchev, B. Dimitrov, & P. Gatev (Eds.), *Motor control* (pp. 183–187). New York: Plenum Press.

An, K. N., Hui, F. C., Morrey, B. F., Linscheid, R. L., & Chao, E. Y. (1981). Muscles across the elbow joint: A biomechanical analysis. *Journal of Biomechanics, 14,* 659–669.

Bizzi, E., Accornero, N., Chapple, W., & Hogan, N. (1984). Posture control and trajectory formation during arm movement. *Journal of Neuroscience, 4,* 2738–2744.

Feldman, A. G. (1966). Functional tuning of the nervous system with control of movement or maintenance of a steady posture. II. Controllable parameters of the muscles. *Biophysics, 11,* 565–578.

Feldman, A. G. (1980). Superposition of motor programs. II. Rapid forearm flexion in man. *Neuroscience, 5,* 91–95.

Feldman, A. G. (1986). Once more on the equilibrium-point hypothesis (λ model) for motor control. *Journal of Motor Behavior, 18,* 17–54.

Feldman, A. G., Adamovich, S. V., Ostry, D. J., & Flanagan, J. R. (1990). The origins of electromyograms—Explanations based on the equilibrium point hypothesis. In J. Winters & S. Woo (Eds.), *Multiple muscle systems: Biomechanics and movement organization* (pp. 195–212). New York: Springer-Verlag.

Flanagan, J. R., Feldman, A. G., & Ostry, D. J. (1992). Equilibrium trajectories underlying rapid target-directed arm movements. In G. E. Stelmach & J. Requin (Eds.), *Tutorials in motor behavior II* (pp. 661–676). Amsterdam: North-Holland.

Flash, T. (1987). The control of hand equilibrium trajectories in multi-joint arm movements. *Biological Cybernetics, 57,* 57–74.

Flash, T., & Henis, E. (1991). Arm trajectory modification during reaching towards visual targets. *Journal of Cognitive Neuroscience, 3,* 220–230.

Gielen, C. C. A. M., Heuvel, P. J. M. van den, & Denier van der Gon, J. J. (1984). Modification of muscle activation patterns during fast goal-directed arm movements. *Journal of Motor Behavior, 16,* 2–19.

Georgopoulos, A. P., Kalaska, J. F., & Massey, J. T. (1981). Spatial trajectories and reaction times of aimed movements: Effects of practice, uncertainty, and change in target location. *Journal of Neurophysiology, 46,* 725–743.

Hill, A. V. (1938). The heat of shortening and the dynamic constants of muscles. *Proceedings of the Royal Society (London), B126,* 136–195.

Hogan, N. (1984). An organizing principle for a class of voluntary movements. *Journal of Neuroscience, 4,* 2745–2754.

Hollerbach, J. M., & Flash, T. (1982). Dynamic interactions between limb segments during planar arm movement. *Biological Cybernetics, 44,* 67–77.

Massey, J. T., Caminiti, R., Schwartz, A. B., & Georgopoulos, A. P. (1986). On information processing and performing a movement sequence. In H. Heuer & C. Fromm (Eds.), *Generation and modulation of action patterns. Experimental Brain Research Series* (Vol. 15, pp. 242-251). Berlin: Springer-Verlag.

Megaw, E. D. (1974). Possible modification to a rapid on-going programmed manual response. *Brain Research, 71,* 425–441.

Milner, T. E. (1992). A model for the generation of movements requiring endpoint precision. *Neuroscience, 49,* 487–496.

Munhall, K. G., & Löfqvist, A. (1992). Gestural aggregation in speech: Laryngeal gestures. *Journal of Phonetics, 20,* 111–126.

Paulignan, Y., MacKenzie, C., Marteniuk, R., & Jeannerod, M. (1991). Selective perturbation of visual input during prehension movements. 1. The effects of changing object position. *Experimental Brain Research, 83,* 502–512.

Péllison, D., Prablanc, C., Goodale, M. A., & Jeannerod, M. (1986). Visual control of reaching movements without vision of the limb. II. Evidence of fast unconscious processes correcting the trajectory of the hand to the final position of a double-step stimulus. *Experimental Brain Research, 62,* 303–311.

Soechting, J. F., & Lacquaniti, F. (1981). Invariant aspects of a pointing movement in man. *Journal of Neuroscience, 1,* 710–720.

Soechting, J. F., & Lacquaniti, F. (1983). Modification of trajectory of a pointing movement in response to a change in target location. *Journal of Neurophysiology, 49,* 548–564.

Van Sonderen, J. F., & Denier van der Gon, J. J. (1990). A simulation study of a programme generator for centrally programmed fast two-joint arm movements: Responses to single- and double-step displacements. *Biological Cybernetics, 63,* 35–44.

Van Sonderen, J. F., Gielen, C. C. A. M., & Denier van der Gon, J. J. (1989). Motor programmes for goal-directed movements are continuously adjusted according to changes in target location. *Experimental Brain Research, 78,* 139–146.

Winter, D. A. (1979). *Biomechanics of human movements.* New York: Wiley.

Submitted January 23, 1992
Revised August 21, 1992
Second revision January 6, 1993